

1 Partitioning plant spectral diversity into 2 alpha and beta components

3 Etienne Laliberté^{1,2*}, Anna K. Schweiger^{1,2}, Pierre Legendre²

4

5 ¹Institut de recherche en biologie végétale, Université de Montréal, 4101 Sherbrooke Est,
6 Montréal, Québec H1X 2B2, Canada

7 ²Département de sciences biologiques, Université de Montréal, C. P. 6128, succursale Centre-
8 ville, Montréal, Québec H3C 3J7, Canada

9 *Corresponding author. Email: etienne.laliberte@umontreal.ca

10 Phone: +1 514 343 6132

11

12 **Running title:** Spectral alpha, beta, and gamma diversity

13 **Keywords:** remote sensing, imaging spectroscopy, spectral variation hypothesis, spectral
14 heterogeneity, alpha diversity, beta diversity, gamma diversity, spectranomics

15 **Type of article:** Methods

16 **Number of words:** 152 (abstract), 5062 (main text, excluding abstract, acknowledgements
17 references, table and figure legends).

18 **Number of references:** 49

19 **Number of figures:** 5

20 **Number of tables:** 1

21 **Statement of authorship:** EL conceived the ideas and performed the analyses. EL and AKS
22 wrote the manuscript. AKS and PL contributed to the ideas, and PL contributed to the writing.

23 **Data statement:** The data supporting the results are archived on Dryad:
24 <https://doi.org/10.5061/dryad.gxd2547gd>

25 **ABSTRACT**

26 Plant spectral diversity — how plants differentially interact with solar radiation — is an integrator
27 of plant chemical, structural, and taxonomic diversity that can be remotely sensed. We propose
28 to measure spectral diversity as spectral variance, which allows the partitioning of the spectral
29 diversity of a region, called spectral *gamma* (γ) diversity, into additive alpha (α ; within
30 communities) and beta (β ; among communities) components. Our method calculates the
31 contributions of individual bands or spectral features to spectral γ -, β -, and α -diversity, as well
32 as the contributions of individual plant communities to spectral diversity. We present two case
33 studies illustrating how our approach can identify “hotspots” of spectral α -diversity within a
34 region, and discover spectrally unique areas that contribute strongly to β -diversity. Partitioning
35 spectral diversity and mapping its spatial components has many applications for conservation
36 since high local diversity and distinctiveness in composition are two key criteria used to
37 determine the ecological value of ecosystems.

38 INTRODUCTION

39 Major environmental changes, including land-use change, climate change, and invasive species
40 are altering the Earth's biodiversity. The rapid rate and broad extent of those changes far
41 exceed our capacity to monitor them via field-based sampling alone. This calls for the
42 development of new remote sensing approaches that can provide rapid estimates of biodiversity
43 over broad regions (Pereira *et al.* 2013; Turner 2014; Bush *et al.* 2017). For terrestrial plants,
44 imaging spectroscopy is emerging as the most promising remote sensing method for estimating
45 biodiversity (Féret & Asner 2014; Wang & Gamon 2019). This is because its high spectral
46 resolution allows plant species to be discriminated from one another, while also enabling the
47 determination of ecologically important foliar functional traits (Asner & Martin 2009; Ustin *et al.*
48 2009).

49 For every pixel of an aerial image, imaging spectroscopy measures reflected solar radiation in
50 tens to hundreds of contiguous, narrow (~10 nm wide) wavelength bands, usually covering all or
51 part of the visible to shortwave infrared range (400–2500 nm) of the electromagnetic spectrum.
52 Leaf “spectral signatures” of plants provide unique expressions among species of how solar
53 radiation interacts with photosynthetic pigments, water, proteins, as well as structural and
54 chemical defense compounds, and thus represent the evolution of plant adaptations to different
55 environmental conditions (Cavender-Bares *et al.* 2016; McManus *et al.* 2016). At the crown
56 scale, these spectral signatures are further influenced by architectural traits due to scattering of
57 photons within canopies (Asner 1998; Ollinger 2010). Therefore, plant spectral diversity is
58 emerging as an integrator of plant chemical, structural and taxonomic diversity that can be
59 remotely sensed (Cavender-Bares *et al.* 2017; Schweiger *et al.* 2018; see also Appendix S1 in
60 Supporting Information).

61 One of the most influential conceptual developments in community ecology has been
62 Whittaker's (1960, 1972) suggestion to partition biodiversity across space into α , β , and γ
63 components. Originally, α diversity was defined as the species diversity *within* communities, and
64 β as the variation in species composition *among* communities; together, α - and β -diversities
65 jointly determined γ -diversity, which is the species diversity across an entire region of interest. In
66 this paper, we transpose this foundational ecological concept from species diversity to spectral
67 diversity (Fig. 1). This requires that the spatial resolution of the imagery matches the size of the
68 object of interest (Woodcock & Strahler 1987), meaning that pixels should be approximately
69 equal or smaller than the size of an average canopy plant. At such fine spatial resolutions, the
70 relationship between spectral and taxonomic diversity is strongest (Wang *et al.* 2018a) and
71 imaging spectroscopy can provide direct, spatially explicit estimates of plant alpha (α ; within
72 community) diversity (Féret & Asner 2014; Wang *et al.* 2018b), and can detect changes in plant
73 community composition across landscapes (Draper *et al.* 2019). The ability to generate wall-to-
74 wall, high-resolution maps of canopy plant diversity across entire regions brings tremendous
75 benefits for biodiversity science and conservation (e.g., Asner *et al.* 2017); however, conceptual
76 and methodological challenges remain, especially with regard to β -diversity estimation (Rocchini
77 *et al.* 2010, 2018).

78 Spectral diversity is sometimes called spectral heterogeneity or spectral variability (Rocchini *et*
79 *al.* 2010), and has been defined as spatial variation in spectral reflectance (Rocchini *et al.* 2010;
80 Ustin & Gamon 2010; Gholizadeh *et al.* 2018; Wang & Gamon 2019). Intuitively, spectral
81 diversity can be conceptualized as multivariate dispersion, for which there are various statistical
82 measures highlighting different aspects of spectral diversity. For example, Wang *et al.* (2018a)
83 used the average coefficient of variation (CV) of each band for a set of pixels, whereas Rocchini
84 *et al.* (2010) used the mean distance from the spectral centroid; we note that the latter has also
85 been proposed as a measure of functional diversity in multivariate trait space (Laliberté &

86 Legendre 2010). However, none of the currently used metrics allow the partitioning of spectral
87 diversity into its α (within communities) and β (among communities) components (Fig. 1).

88 Here we propose to use the *spectral variance* among image pixels as a measure of spectral
89 diversity. Our approach builds on that of Legendre and De Cáceres (2013) for species inventory
90 data, adapts it to spectral data, and extends it to jointly consider α -, β -, and γ -diversity. Casting
91 spectral diversity as spectral variance has a number of benefits:

- 92 1. the classical partitioning of sums of squares allows us to partition spectral γ -diversity into
93 additive spectral α - and β -diversity components (Fig. 1), from which the relative
94 importance of local and regional processes regulating spectral diversity across a region
95 of interest can be inferred;
- 96 2. it allows us to estimate the contributions of individual plots or communities to spectral β -
97 diversity, highlighting areas that are spectrally distinct within the broader region;
- 98 3. it allows us to calculate the contributions of individual bands or spectral features to
99 spectral γ -, β - or α -diversity (Fig. 2), providing information about the underlying biological
100 traits driving spectral diversity;
- 101 4. it is easily implemented in software packages in a computationally efficient way, which is
102 important when dealing with high-volume image data;
- 103 5. it provides a direct link to other statistical procedures based on least squares (e.g.,
104 MANOVA, multiple linear regression, canonical redundancy analysis, K -means
105 partitioning).

106 After describing the theory behind our spectral diversity partitioning approach, we illustrate it
107 using a simulation. We then apply our method to imaging spectroscopy data collected over the
108 Bartlett Experimental Forest by the National Ecological Observatory Network (NEON) Airborne

109 Observation Platform (AOP; Kampe *et al.* 2010). The R code and data for our analyses are
110 available online (<https://github.com/elaliberte/specdiv>).

111 **PARTITIONING SPECTRAL DIVERSITY**

112 **Size and shape of spatial units**

113 Partitioning spectral γ -diversity into its α and β components first requires defining the extent of
114 the region of interest (Fig. 1). Delineating the region of interest is relatively straightforward since
115 it corresponds to the region over which imagery is acquired or a subset thereof. Delineating the
116 size and shape of communities across the region of interest, however, is more difficult. What
117 constitutes an ecological community has been the subject of considerable debate (see review
118 by Ricklefs 2008). Generally, a community is defined as “a group of organisms representing
119 multiple species living in a specified place and time” (Vellend 2010). This definition implies that
120 a community must be larger than the size of an individual organism, but how much larger will
121 depend on the objectives of the study. For the purpose of this work, we focus on communities of
122 canopy plants, because these are the organisms that can be seen in aerial images. We use
123 “community” in the sense of “sampling unit” in vegetation surveys, which can be defined as the
124 area in which the species composition of the vegetation type of interest is adequately
125 represented (Mueller-Dombois & Ellenberg 1974).

126 Setting the size of a community to the size of typical inventory plot for a given ecosystem type
127 facilitates interpretation as this is the sampling unit that field ecologists are familiar with. For
128 example, forest inventory plots often measure 20 m \times 20 m (Fig. 1), which is large enough to
129 include several canopy trees. However, we recognize that setting fixed and regularly shaped
130 boundaries to delineate communities is artificial (Ricklefs 2008), and point out that community
131 size and shape can be changed in the analysis.

132 Spectral gamma (γ) diversity

133 Let $\mathbf{Y} = [y_{ij}]$ be a matrix containing the positions, along the p axes defining the *spectral space*
134 (column vectors $\mathbf{y}_1, \mathbf{y}_2, \dots, \mathbf{y}_p$ of \mathbf{Y}), of n pixels (row vectors $\mathbf{x}_1, \mathbf{x}_2, \dots, \mathbf{x}_n$ of \mathbf{Y}) in a region of
135 interest (Fig. 2). We use indices i and j to denote rows (pixels) and columns (axes) of matrix \mathbf{Y} ,
136 respectively. The p axes could be all or a subset of the original spectral bands, a set of
137 vegetation indices calculated from selected spectral bands (Bannari *et al.* 1995), or a set of p
138 uncorrelated spectral features extracted using dimensionality reduction methods such as
139 principal component analysis (PCA). We use PCA in this section and in our case studies and
140 point out the mathematical relationships between the principal components (PCs) and spectral
141 variation below. We use the general term *variation* for sums of squares (SS, an abbreviation for
142 “sum of the squared deviations from the mean”), and reserve the term *variance* when talking
143 about spectral diversity (SD).

144 We refer to the total spectral diversity of the entire region as spectral γ -diversity (SD_γ). SD_γ is
145 measured by the total variance of \mathbf{Y} , or $\text{Var}(\mathbf{Y})$. This is done by first computing for every pixel
146 and spectral feature y_{ij} the squared deviations s_{ij} from the average pixel (across the whole
147 region) in terms of spectral reflectance, i.e. the column means of \mathbf{Y} :

$$s_{ij} = (y_{ij} - \bar{y}_j)^2. \quad (1)$$

148 The total sum of squares (SS) of matrix \mathbf{Y} is calculated by summing all s_{ij} :

$$SS_\gamma = \sum_{i=1}^n \sum_{j=1}^p s_{ij}. \quad (2)$$

149 Contrary to SS_γ , SD_γ is scaled by the number of pixels in the region, such that SD_γ of regions
150 containing different numbers of pixels can be compared with one another:

$$SD_\gamma = \text{Var}(\mathbf{Y}) = SS_\gamma / (n - 1). \quad (3)$$

151 We note that for calculating the joint SD_γ of adjacent regions, their SS_γ statistics can be added
152 and divided by the total number of pixels minus one, but their region-level SD_γ statistics cannot
153 be added directly.

154 One might be interested in determining the individual contribution of the j th spectral feature to
155 SS_γ . We call this the *feature contribution to spectral γ -diversity* or $FCSD_{\gamma,j}$ (Fig. 2), which can be
156 calculated from the sum of squares of the j th feature:

$$SS_{\gamma,j} = \sum_{i=1}^n s_{ij}. \quad (4)$$

157 Dividing $SS_{\gamma,j}$ by $(n - 1)$ gives the variance of the j th feature, or $\text{Var}(\mathbf{y}_j)$. $FCSD_{\gamma,j}$ can then be
158 calculated as:

$$FCSD_{\gamma,j} = \text{Var}(\mathbf{y}_j)/\text{Var}(\mathbf{Y}) = SS_{\gamma,j}/SS_\gamma. \quad (5)$$

159 If the p features are principal components from PCA scaling type 1, then the $FCSD_{\gamma,j}$ values
160 correspond to their relative eigenvalues. We note that $FCSD_{\gamma,j}$ cannot be mapped because the
161 contribution of each spectral feature applies to the region as a whole.

162 Likewise, one might wish to estimate the individual contribution of the i th pixel within the region
163 to SD_γ . We refer to this as the *local contribution to spectral γ -diversity*, or $LCSD_{\gamma,i}$, which is
164 calculated as:

$$LCSD_{\gamma,i} = SS_{\gamma,i}/SS_\gamma \quad (6)$$

165 where

$$SS_{\gamma,i} = \sum_{j=1}^p s_{ij}. \quad (7)$$

166 We note that $LCSD_{\gamma,i}$ indices are important visual elements in PCA ordination: each $LCSD_{\gamma,i}$
167 value corresponds to the squared distance from one pixel to the centroid in the p -dimensional
168 PCA ordination plot. In addition, the $LCSD_{\gamma,i}$ can be plotted on maps since one value is
169 associated with every pixel in the image. Doing so indicates which pixels are most spectrally

170 dissimilar from the mean pixel of the region in spectral feature space. We note that the $SS_{\gamma,i}$ and
171 $LCSD_{\gamma,i}$ indices are additive. The indices from adjacent pixels within an area of interest, for
172 example an individual tree, can be added up, such that their sums represent the local
173 contributions of the area of interest to SS_{γ} and SD_{γ} . LCSD indices are also useful when
174 computed at the community scale (i.e. $LCSD_{\beta}$), because they then correspond to the ecological
175 concept of β -diversity; see “Spectral beta (β) diversity” below.

176 **Partitioning the total sum of squares**

177 Partitioning the sum of squares forms the basis of a series of classic statistical approaches
178 based on least squares, such as the analysis of variance (ANOVA). From these methods, it is
179 well known that the total sum of squares of a matrix \mathbf{Y} (SS_{total}) can be partitioned into additive
180 among-group (SS_{among}) and within-group (SS_{within}) components:

$$SS_{\text{total}} = SS_{\text{among}} + SS_{\text{within}}. \quad (8)$$

181 In linear regression analysis, we talk about the SS explained by the regression equation and the
182 residual variation. These two components sum to the total sum of squares.

183 Using the same indices as in the previous section, the ANOVA relationship can be expressed
184 as:

$$\sum_{i=1}^n \sum_{j=1}^p (y_{ij} - \bar{y}_j)^2 = \sum_{k=1}^q \sum_{j=1}^p m (\hat{y}_{kj} - \bar{y}_j)^2 + \sum_{i=1}^m \sum_{k=1}^q \sum_{j=1}^p (y_{ij} - \hat{y}_{kj})^2 \quad (9)$$

185 where q is the number of groups, \hat{y}_{kj} is the arithmetic mean of the j th variable (column) for the
186 k th group:

$$\hat{y}_{kj} = \left(\sum_{i=1}^m y_{ijk} \right) / m \quad (10)$$

187 and where m is the number of samples (rows) in each group k ; an important assumption here is
188 that m is equal in each group. The proof of this theorem can be found in standard statistics
189 textbooks and is therefore not shown here.

190 In the next two sections, we apply Equation 9 to partition the total sum of squares of a region
191 SS_Y into additive among- (β) and within-group (α) components from which spectral β - and α -
192 diversity can be calculated directly.

193 **Spectral beta (β) diversity**

194 Let us divide \mathbf{Y} into q groups of m spatially contiguous pixels, where each group corresponds to
195 a local community (e.g., a vegetation survey plot); $n = q m$. Here, we assume that each of these
196 communities corresponds to a square of equal area, which is \sqrt{m} pixels wide; with this setup,
197 each community is represented by the same number of pixels. We will present later our
198 suggestion to use a rarefaction procedure to handle situations where m differs among groups.
199 *Spectral β -diversity*, or SD_β , represents the degree to which the q communities within a region
200 differ from each other in terms of spectral composition. We note that SD_β is a *non-directional*
201 *measure of β -diversity sensu Anderson et al. (2011)*. To calculate SD_β , we first compute the
202 squared deviations s_{kj} of the k th community from the average pixel of the region in terms of
203 spectral reflectance, i.e. the column means of \mathbf{Y} across all variables j :

$$s_{kj} = (\hat{y}_{kj} - \bar{y}_j)^2 \quad (11)$$

204 where \hat{y}_{kj} is the arithmetic mean of the k th community (i.e. the community centroid) for the j th
205 spectral feature (Equation 10).

206 The sum of squares associated with each community k ($SS_{\beta,k}$) is:

$$SS_{\beta,k} = \sum_{j=1}^p m s_{kj}. \quad (12)$$

207 The total sum of squares of the β component (SS_{β}) is:

$$SS_{\beta} = \sum_{k=1}^q SS_{\beta,k} \quad (13)$$

208 from which SD_{β} is calculated as:

$$SD_{\beta} = SS_{\beta}/(n - 1). \quad (14)$$

209 The contribution of each community k to SD_{β} , which we call the *local contribution to spectral β -*
210 *diversity* ($LCSD_{\beta,k}$), can be computed by the following ratio of sum of squares:

$$LCSD_{\beta,k} = SS_{\beta,k}/SS_{\beta}. \quad (15)$$

211 Finally, one can compute the *feature contribution to spectral β -diversity* or $FCSD_{\beta,j}$ of the j th
212 spectral feature as:

$$FCSD_{\beta,j} = SS_{\beta,j}/SS_{\beta} \quad (16)$$

213 where

$$SS_{\beta,j} = \sum_{k=1}^q m s_{kj}. \quad (17)$$

214 We note here that $LCSD_{\beta,k}$ can be mapped because each community k has its own $LCSD_{\beta}$
215 value. On the other hand, $FCSD_{\beta,j}$ or SD_{β} cannot be mapped because they refer to the region as
216 a whole.

217 **Spectral alpha (α) diversity**

218 Spectral α -diversity, or SD_{α} , is the degree to which neighbouring pixels *within* a local community
219 differ spectrally from each other. Contrary to SD_{β} and SD_{γ} , which apply to the entire region, SD_{α}
220 is defined at the community level. Therefore, we denote SD_{α} by the index k , $SD_{\alpha,k}$, since it is
221 measured for each community k . To calculate $SD_{\alpha,k}$, we first compute for every pixel and

222 spectral feature per community y_{ijk} the squared deviations s_{ijk} from the mean pixel spectrum of
223 the k th community for each spectral feature or column of \mathbf{Y} :

$$s_{ijk} = (y_{ijk} - \hat{y}_{kj})^2. \quad (18)$$

224 The sum of squares associated with the j th spectral feature of community k is:

$$SS_{\alpha,jk} = \sum_{i=1}^m s_{ijk}, \quad (19)$$

225 and the total sum of squares for community k is:

$$SS_{\alpha,k} = \sum_{j=1}^p \sum_{i=1}^m s_{ijk}. \quad (20)$$

226 $SD_{\alpha,k}$ is obtained by dividing $SS_{\alpha,k}$ by $(m - 1)$, where m is the number of pixels within one
227 community, to make it comparable with other communities differing in their numbers of pixels:

$$SD_{\alpha,k} = SS_{\alpha,k} / (m - 1). \quad (21)$$

228 The total sum of squares of the α -component for all q communities within the entire region is:

$$SS_{\alpha} = \sum_{k=1}^q SS_{\alpha,k}. \quad (22)$$

229 Importantly, following Equations 8 and 9, SS_{α} and SS_{β} are linked to SS_{γ} by the relationship:

$$SS_{\gamma} = SS_{\beta} + SS_{\alpha}. \quad (23)$$

230 Therefore, SS_{α} and SS_{β} can be used directly to determine the relative importance of the α and β
231 components to spectral γ -diversity.

232 Finally, the *contribution of the j th feature to the spectral α -diversity* of the k th community, which
233 we call $FCSD_{\alpha,jk}$, can be computed as:

$$FCSD_{\alpha,jk} = SS_{\alpha,jk} / SS_{\alpha,k}. \quad (24)$$

234 These $FCSD_{\alpha,jk}$ values can be mapped and give us useful information about the origin of
235 spectral α -diversity across different communities.

236 CASE STUDY 1: SIMULATED REGIONS

237 To illustrate our approach, we first use leaf spectra data to simulate imagery (Appendix S2).

238 This removes much of the complexity associated with real imagery, where one has to deal with
239 much higher numbers of pixels, varying illumination and sensor viewing geometry, and
240 presence of shaded and non-vegetated pixels. We simulated two regions with equal spectral γ -
241 diversity, but contrasting spectral β - and α -diversities (Fig. 3). Each region is composed of $25 \times$
242 25 pixels, populated with leaf-level spectra of three temperate tree species (i.e. *Populus*
243 *deltoides* W. Bartram ex Marshall subsp. *deltoides* Marsh, *P. tremuloides* Michaux, and *Betula*
244 *alleghaniensis* Britton) measured in the field on 15 individual plants (Fig. S1). These 25×25
245 pixels regions are equally split into 25 communities, each composed of 5×5 pixels.

246 For both scenarios, we calculated the SS across the entire region (SS_γ), partitioned SS_γ into its
247 β and α components, and calculated spectral γ - β -, and α -diversity (Fig. 4a). As spectral
248 features (columns of \mathbf{Y}) we used the first three PCs (using type-I scaling in PCA), which
249 together explained >97% of the total variation in spectral reflectance. As expected, spectral γ -
250 diversity was equal for both scenarios (Table 1), whether expressed as the total sum of squares
251 ($SS_\gamma = 1.66$), or standardized by $n - 1$ pixels ($SD_\gamma = 0.0027$). In addition, in the high β -diversity
252 scenario, spectral variation among communities (SS_β , ~84%) largely exceeded spectral
253 variation within communities (SS_α , ~16%), whereas in the low β -diversity scenario SS_β was
254 much lower (~5%) than SS_α (~95%) (Table 1).

255 Next, we determined the local contributions of individual communities to spectral β -diversity
256 (LCSD $_\beta$). In the high β -diversity scenario (Fig. 4b, left panel), communities 12 and 21 (numbered
257 as in Fig. 3) contributed the most to spectral β -diversity. These were the only two plots (out of
258 25) containing spectra of *Populus tremuloides*. In other words, these two plots had the most
259 distinctive spectral composition compared to other communities. By contrast, in the low β -

260 diversity scenario, community 16 was the most spectrally distinct community, something that
261 could not be easily detected by examining this scenario visually (Fig. 3, right panel). As
262 illustrated here, it is important to note that a region with low SD_{β} can still have individual
263 communities showing high $LCSD_{\beta}$ values, because $LCSD_{\beta}$ values are *proportions* of SD_{β} .

264 We then estimated the contributions of individual spectral features to spectral diversity (FCSD)
265 for each scenario. For spectral γ -diversity (total variance of the region), $FCSD_{\gamma}$ declined
266 progressively from the first to the third PC (Table 1). As mentioned previously, $FCSD_{\gamma}$ values are
267 equal to the relative PCA eigenvalues of the spectral feature. Likewise, for spectral β -diversity,
268 the contribution from the first to subsequent PCs decreased in both scenarios (Table 1). The
269 relative contributions of individual spectral features to β -diversity were fairly similar in both
270 regions, even though they differed considerably in spectral β -diversity. For spectral α -diversity,
271 however, $FCSD_{\alpha}$ values differed noticeably among the two scenarios (Fig. 4c–d). In the low α -
272 diversity scenario (Fig. 4c-d, left column), PC 2 contributed more strongly to the spectral α -
273 diversity of most communities than PC 1, whereas the opposite was true for the high α -diversity
274 scenario (Fig. 4c–d, right column). The $FCSD_{\alpha}$ values were not expected to decrease in a
275 monotonic way since α -diversity is orthogonal to γ -diversity and the PCs are those of γ -, not of
276 α -diversity.

277 We note that SS, SD and LCSD indices are exactly the same whether using the original spectral
278 bands or all PCs, because PCA type-I scaling preserves the Euclidean distance among objects
279 (e.g., image pixels in spectral space). Conversely, the equations developed in this paper hold
280 and can be used directly with the original band data. However, FCSD values would change
281 when using the original spectral bands instead of PCs, since this would then indicate the relative
282 contributions of individual spectral bands (instead of PCs) to spectral diversity.

283 **CASE STUDY 2: NEON IMAGERY**

284 Next, we applied our method for partitioning spectral diversity to imaging spectroscopy data
285 collected by NEON's Airborne Observation Platform (AOP; Kampe *et al.* 2010) over the Bartlett
286 Experimental Forest (<https://www.neonscience.org/field-sites/field-sites-map/BART>). In this case
287 study, we used a scene measuring 280 m (east-west) x 1000 m (north-south), acquired in
288 August 2017. Spectral data were processed to surface reflectance and subsampled to 1-m pixel
289 size by NEON. Our workflow is illustrated in Figure 2.

290 For spectral diversity calculations we selected a community (i.e. plot) size of 40 m × 40 m, which
291 is the base plot size used by NEON. We used rarefaction to standardize the number of pixels
292 per community used for analysis. We used a normalized difference vegetation index (NDVI)
293 threshold of ≥ 0.8 to identify the minimum number of vegetated pixels across all plots in the
294 image (termed m_{\min}), which was 1474 (= 92% of the 1600 pixels per community). We randomly
295 selected m_{\min} pixels per plot, and applied our spectral diversity partitioning approach to all
296 selected pixels. The rarefaction was repeated 30 times and results were averaged across all 30
297 repeats (Fig. 2). Alternatively, one could take the median value instead of the mean if
298 distributions are skewed.

299 Our analyses revealed that spectral α -diversity in this forested landscape accounted for 77% of
300 the spectral γ -diversity, whereas β -diversity accounted for the remaining 23% (Table 1). In other
301 words, there is considerably more spectral diversity within individual 40 m × 40 m communities
302 than among communities in this forest. Figure 5 illustrates how spectral diversity is spatially
303 structured. Two areas contribute strongly to spectral β -diversity (LCSD $_{\beta}$, darker colours in Fig.
304 5). The tree communities in these areas are more spectrally dissimilar from the average
305 community than communities with lower LCSD $_{\beta}$ (lighter colours in Fig. 5).

306 For completeness, we evaluated the effects of shadows and community size on spectral
307 diversity calculations (Appendix S3). We found that removing shadows had little influence on
308 spectral diversity (Figs. S4–S6) and that results remained remarkably stable for plots ranging
309 from 20 m × 20 m (400 m²) to 140 m × 140 m (almost 2 ha) in size (Figs. S7–S9).

310 **DISCUSSION**

311 In this paper, we proposed a new method for partitioning plant spectral γ -diversity (i.e. the
312 spectral diversity of a region) into additive α - (within community) and β -diversity (among
313 community) components. Our approach builds on a method for partitioning β -diversity initially
314 designed for community data (Legendre & Cáceres 2013), adapts it to spectral data and,
315 importantly, extends it to include α , β and γ components. Partitioning spectral diversity can bring
316 new insights and generate new hypotheses about the origins and maintenance of plant spectral
317 diversity across regions. For instance, high spectral β -diversity could result from turnover in
318 plant species and/or functional trait composition across environmental gradients (e.g., soil
319 properties, hydrology), whereas high spectral α -diversity might result from local biotic
320 interactions among co-occurring plants (e.g., resource partitioning, conspecific negative density
321 dependence). Mapping spectral indices such as LCSD_β and SD_α could be used as a biodiversity
322 “discovery tool” to design targeted field sampling campaigns to test such hypotheses, e.g., by
323 comparing community composition and diversity in areas with high and low LCSD_β and SD_α
324 values, respectively (Fig. 5).

325 Partitioning spectral diversity allows the determination of the spectral features contributing most
326 strongly to spectral α -, β - or γ -diversity (FCSD), which helps in understanding the underlying
327 biological traits driving spectral diversity at different spatial scales. In our case studies, the
328 spectral features were principal components (PCs), which are linear combinations of the original
329 wavelength bands. As such, the individual contributions of all wavelength bands to each

330 spectral feature can be retrieved. The bands, in turn, can be linked to specific plant properties,
331 since the biophysical and biological causes of spectral variation across spectral regions and for
332 specific absorption features of molecules are reasonably well understood (Gates *et al.* 1965;
333 Curran 1989; Asner 1998; Kokaly *et al.* 2009; Ustin *et al.* 2009). Identifying the traits contributing
334 most strongly to spectral α -diversity might inform us about how co-occurring species are
335 partitioning resources at the local scale, whereas identifying the traits contributing most strongly
336 to spectral β -diversity might reveal important mechanisms driving changes in community
337 composition across environmental gradients.

338 Partitioning plant spectral diversity and mapping its spatial components has applications in
339 biodiversity management. Indeed, managers often need to estimate the ecological value of
340 different ecosystems over large regions, for example to prioritize conservation or restoration
341 efforts. However, access to field data might be limited. Using imaging spectroscopy data, our
342 approach of partitioning spectral diversity allows the identification of areas with high spectral α -
343 diversity, which likely coincide with local “hotspots” of taxonomic and/or functional trait diversity.
344 Further, high LCSD $_{\beta}$ values indicates areas with rare spectral composition, i.e., containing
345 communities that are most spectrally dissimilar from the average community within the region of
346 interest. Given that species spectral dissimilarity is linked to their functional and phylogenetic
347 dissimilarity (Schweiger *et al.* 2018), spectrally rare communities can be expected to have rare
348 taxonomic and/or functional composition, either because they harbor uncommon species, or
349 rare combinations of common species.

350 Our approach measures spectral variance directly (Fig. 2), which is in contrast to other studies
351 that have prior to deriving biodiversity metrics first translated remotely-sensed spectra into plant
352 species (e.g., Féret & Asner 2013), “spectral species” (Féret & Asner 2014), or plant functional
353 traits (e.g., Dahlin *et al.* 2013; Schneider *et al.* 2017). While spectral diversity does not isolate
354 any particular facet of plant biodiversity (e.g., taxonomic, chemical, structural), it integrates all of

355 these facets (Schweiger *et al.* 2018; Appendix S1). From a practical perspective, casting
356 spectral diversity as spectral variance depends on fewer user decisions compared to other
357 approaches (e.g., selecting the number of clusters for classifying spectral species, selecting the
358 plant traits and modelling approach to predict traits from spectra). This makes spectral diversity
359 easily comparable across different regions. Therefore, maps of SD_{α} and $LCSD_{\beta}$ could be ideal
360 candidates for biodiversity products from remotely sensed spectral imagery.

361 **Comparison with other approaches**

362 Much of the interest in measuring spectral diversity from remote sensing data stems from the
363 spectral variation hypothesis (Palmer *et al.* 2002), stating that the spatial variation in spectral
364 reflectance expresses overall variation of the environment. As areas of high environmental
365 variation often harbour more species than areas with low environmental variation, spectral
366 variation across space can potentially uncover botanically interesting areas (Palmer *et al.* 2002).
367 However, spectral diversity has been predominantly used to investigate relationships between
368 plant spectra and taxonomic units at the α - and γ -diversity scale, whereas the β component has
369 received less attention (Rocchini *et al.* 2018).

370 Historically, Landsat satellites were instrumental for spurring large-scale biodiversity studies.
371 Early sensors contained few spectral bands; thus, a large body of literature deals with using
372 NDVI for predicting and mapping taxonomic diversity (Gould 2000; see review by Pettorelli *et al.*
373 2005). Recent advances in sensor technology, particularly increased spectral resolution, have
374 led to a variety of approaches to calculate spectral α -diversity (Rocchini *et al.* 2010). This
375 includes metrics such as the standard deviation or coefficient of variation of spectral indices
376 (Oindo & Skidmore 2002), or spectral bands among pixels (Hall *et al.* 2010; Gholizadeh *et al.*
377 2018; Wang *et al.* 2018a), the convex hull volume of pixels in spectral feature space (Dahlin
378 2016), the mean distance of pixels from the spectral centroid (Rocchini *et al.* 2010), the number

379 of spectrally distinct clusters or spectral species in ordination space (Féret & Asner 2014), and
380 diversity metrics based on dissimilarity matrices among species spectra or image pixels
381 (Schweiger *et al.* 2018). Of these, our method is most similar to the mean distance to the
382 spectral centroid (Rocchini *et al.* 2010). The difference is that we square the individual distances
383 to the spectral centroid; doing so allows us to partition sums of squares into additive
384 components (Equation 9).

385 Fewer studies have considered spectral β -diversity (Rocchini *et al.* 2018). One approach for
386 studying β -diversity using spectra has been to combine ordination scores of species inventories
387 with spectral data in multivariate models to predict the positions of pixels with unknown species
388 composition in species-ordination-space (Schmidtlein *et al.* 2007). This method and some of its
389 variants (Rocchini *et al.* 2018) do not measure spectral β -diversity *per se*, but instead use
390 spectra to estimate changes in community composition across the landscape. Rao's quadratic
391 entropy has been suggested as a measure of spectral β -diversity, based on the dissimilarity
392 among image pixels within a moving window (Rocchini *et al.* 2018). However, a moving window
393 approach expresses spectral β -diversity for many small sub-regions independently from one
394 another and does not estimate the spectral β -diversity of the region as a whole. Another
395 approach for studying spectral β -diversity has been to measure the pairwise dissimilarity in the
396 composition of spectral species among mapping units, and to re-project those pairwise
397 dissimilarities onto an RGB colour space (Féret & Asner 2014). This method yields a useful map
398 showing changes in spectral composition across the region, similar to our mapping of the first
399 three PCs in Figure 5, but it does not calculate spectral diversity.

400 **Methodological considerations**

401 A number of methodological aspects should be considered before applying our approach to
402 imaging spectroscopy data. These include: (1) the choice of a brightness normalization

403 procedure, (2) whether all or a subset of the wavelength bands, or spectral features, should be
404 used, (3) masking non-vegetated pixels, or not, (4) determining community size, and (5)
405 deciding on the scaling type (i.e. type I or II; Legendre & Legendre 2012) if using PCA as a
406 spectral feature extraction method. We discuss these methodological points in detail in
407 Appendix S4.

408 **CONCLUSION**

409 Plant spectral diversity is emerging as an integrator of chemical, structural, and taxonomic
410 aspects of plant biodiversity, which can be remotely sensed (Cavender-Bares *et al.* 2017).
411 Partitioning plant spectral diversity using our approach can help us to better understand and
412 generate new hypotheses about the origins of, and the processes that drive, biodiversity
413 variation across regions. Given the rapid and broad extent of current environmental changes,
414 remote sensing of plant biodiversity over large regions is more important than ever (Turner
415 2014; Wang & Gamon 2019). Our approach can identify local α -diversity hotspots as well as
416 unique areas contributing strongly to β -diversity – two central facets of biodiversity.

417 Our approach is timely since current technological developments in high-resolution UAV
418 imaging spectroscopy will make this technology more accessible to ecologists in the coming
419 years (Aasen *et al.* 2018; Arroyo-Mora *et al.* 2019). For example, the Canadian Airborne
420 Biodiversity Observatory (www.caboscience.org) is developing UAV spectroscopy to understand
421 how plant biodiversity is responding to major environmental changes across Canada. We
422 anticipate that a growing number of ecologists will embrace this transformative technology for
423 mapping plant biodiversity. In fact, a wealth of moderate-resolution imaging spectroscopy data
424 are already freely available for a wide range of ecosystems across the United States as part of
425 the NEON program (www.neonscience.org). Partitioning spectral diversity could become a
426 useful tool for remotely sensing plant biodiversity from these new data sources.

427 **ACKNOWLEDGEMENTS**

428 EL was supported by a Discovery Grant from the Natural Sciences and Engineering Research
429 Council of Canada (NSERC; Grant numbers RGPIN-2014-06106, RGPIN-2019-04537). PL was
430 supported by NSERC Discovery Grant number 7738. Teaching relief to EL that facilitated the
431 writing of this manuscript was provided by the Canada Research Chair (CRC) in Plant
432 Functional Biodiversity, and by Université de Montréal (UdeM) in support of a Discovery
433 Frontiers grant from NSERC (Grant number 509190-2017) to EL to establish the Canadian
434 Airborne Biodiversity Observatory (CABO). AKS was supported by a postdoctoral fellowship
435 from CABO. EL wishes to thank colleagues from CABO and graduate students from the
436 Laboratory of Plant Functional Ecology (LEFO) at UdeM for stimulating discussions about
437 remote sensing of plant biodiversity, which helped to shape some of the ideas presented here.

438 REFERENCES

- 439 Aasen, H., Honkavaara, E., Lucieer, A., Zarco-Tejada, P., Aasen, H., Honkavaara, E., *et al.*
440 (2018). Quantitative remote sensing at ultra-high resolution with UAV spectroscopy: a review of
441 sensor technology, measurement procedures, and data correction workflows. *Remote Sens.*,
442 10, 1091.
- 443 Anderson, M.J., Crist, T.O., Chase, J.M., Vellend, M., Inouye, B.D., Freestone, A.L., *et al.*
444 (2011). Navigating the multiple meanings of β diversity: a roadmap for the practicing ecologist.
445 *Ecol. Lett.*, 14, 19–28.
- 446 Arroyo-Mora, J.P., Kalacska, M., Inamdar, D., Soffer, R., Lucanus, O., Gorman, J., *et al.* (2019).
447 Implementation of a UAV–hyperspectral pushbroom imager for ecological monitoring. *Drones*,
448 3, 12.
- 449 Asner, G.P. (1998). Biophysical and biochemical sources of variability in canopy reflectance.
450 *Remote Sens. Environ.*, 64, 234–253.
- 451 Asner, G.P. & Martin, R.E. (2009). Airborne spectranomics: mapping canopy chemical and
452 taxonomic diversity in tropical forests. *Front. Ecol. Environ.*, 7, 269–276.
- 453 Asner, G.P., Martin, R.E., Knapp, D.E., Tupayachi, R., Anderson, C.B., Sinca, F., *et al.* (2017).
454 Airborne laser-guided imaging spectroscopy to map forest trait diversity and guide conservation.
455 *Science*, 355, 385–389.
- 456 Bannari, A., Morin, D., Bonn, F. & Huete, A.R. (1995). A review of vegetation indices. *Remote*
457 *Sens. Rev.*, 13, 95–120.
- 458 Bush, A., Sollmann, R., Wilting, A., Bohmann, K., Cole, B., Balzter, H., *et al.* (2017). Connecting
459 Earth observation to high-throughput biodiversity data. *Nat. Ecol. Evol.*, 1, s41559-017-0176–
460 017.

- 461 Cavender-Bares, J., Gamon, J.A., Hobbie, S.E., Madritch, M.D., Meireles, J.E., Schweiger, A.K.,
462 *et al.* (2017). Harnessing plant spectra to integrate the biodiversity sciences across biological
463 and spatial scales. *Am. J. Bot.*, 104, 966–969.
- 464 Cavender-Bares, J., Meireles, J.E., Couture, J.J., Kaproth, M.A., Kingdon, C.C., Singh, A., *et al.*
465 (2016). Associations of leaf spectra with genetic and phylogenetic variation in oaks: prospects
466 for remote detection of biodiversity. *Remote Sens.*, 8, 221.
- 467 Curran, P.J. (1989). Remote sensing of foliar chemistry. *Remote Sens. Environ.*, 30, 271–278.
- 468 Dahlin, K.M. (2016). Spectral diversity area relationships for assessing biodiversity in a
469 wildland–agriculture matrix. *Ecol. Appl.*, 26, 2758–2768.
- 470 Dahlin, K.M., Asner, G.P. & Field, C.B. (2013). Environmental and community controls on plant
471 canopy chemistry in a Mediterranean-type ecosystem. *Proc. Natl. Acad. Sci.*, 110, 6895–6900.
- 472 Draper, F.C., Baraloto, C., Brodrick, P.G., Phillips, O.L., Martinez, R.V., Coronado, E.N.H., *et al.*
473 (2019). Imaging spectroscopy predicts variable distance decay across contrasting Amazonian
474 tree communities. *J. Ecol.*, 107, 696–710.
- 475 Feilhauer, H., Asner, G.P., Martin, R.E. & Schmidtlein, S. (2010). Brightness-normalized partial
476 least squares regression for hyperspectral data. *J. Quant. Spectrosc. Radiat. Transf.*, 111,
477 1947–1957.
- 478 Féret, J.B. & Asner, G.P. (2013). Tree species discrimination in tropical forests using airborne
479 imaging spectroscopy. *IEEE Trans. Geosci. Remote Sens.*, 51, 73–84.
- 480 Féret, J.-B. & Asner, G.P. (2014). Mapping tropical forest canopy diversity using high-fidelity
481 imaging spectroscopy. *Ecol. Appl.*, 24, 1289–1296.
- 482 Gates, D.M., Keegan, H.J., Schleter, J.C. & Weidner, V.R. (1965). Spectral properties of plants.
483 *Appl. Opt.*, 4, 11–20.

- 484 Gholizadeh, H., Gamon, J.A., Zyguelbaum, A.I., Wang, R., Schweiger, A.K. & Cavender-Bares,
485 J. (2018). Remote sensing of biodiversity: Soil correction and data dimension reduction methods
486 improve assessment of α -diversity (species richness) in prairie ecosystems. *Remote Sens.*
487 *Environ.*, 206, 240–253.
- 488 Gould, W. (2000). Remote sensing of vegetation, plant species richness, and regional
489 biodiversity hotspots. *Ecol. Appl.*, 10, 1861–1870.
- 490 Hall, K., Johansson, L.J., Sykes, M.T., Reitalu, T., Larsson, K. & Prentice, H.C. (2010).
491 Inventorying management status and plant species richness in semi-natural grasslands using
492 high spatial resolution imagery. *Appl. Veg. Sci.*, 13, 221–233.
- 493 Kampe, T.U., Johnson, B.R., Kuester, M. & Keller, M. (2010). NEON: the first continental-scale
494 ecological observatory with airborne remote sensing of vegetation canopy biochemistry and
495 structure. *J. Appl. Remote Sens.*, 4, 043510-043510–24.
- 496 Kokaly, R.F., Asner, G.P., Ollinger, S.V., Martin, M.E. & Wessman, C.A. (2009). Characterizing
497 canopy biochemistry from imaging spectroscopy and its application to ecosystem studies.
498 *Remote Sens. Environ.*, 113, 78–91.
- 499 Laliberté, E. & Legendre, P. (2010). A distance-based framework for measuring functional
500 diversity from multiple traits. *Ecology*, 91, 299–305.
- 501 Legendre, P. & Cáceres, M.D. (2013). Beta diversity as the variance of community data:
502 dissimilarity coefficients and partitioning. *Ecol. Lett.*, 16, 951–963.
- 503 Legendre, P. & Legendre, L. (2012). *Numerical Ecology*. 3rd English edition. Elsevier Science,
504 Amsterdam, Netherlands.
- 505 McManus, K.M., Asner, G.P., Martin, R.E., Dexter, K.G., Kress, W.J. & Field, C.B. (2016).
506 Phylogenetic structure of foliar spectral traits in tropical forest canopies. *Remote Sens.*, 8, 196.

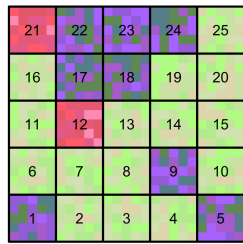
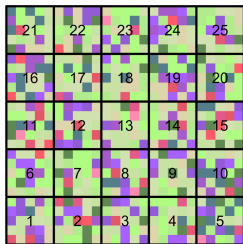
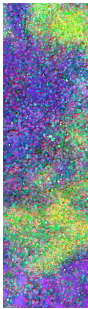
- 507 Mueller-Dombois, D. & Ellenberg, H. (1974). *Aims and Methods of Vegetation Ecology*. John
508 Wiley & Sons, Inc., New York, USA.
- 509 Oindo, B.O. & Skidmore, A.K. (2002). Interannual variability of NDVI and species richness in
510 Kenya. *Int. J. Remote Sens.*, 23, 285–298.
- 511 Ollinger, S.V. (2010). Sources of variability in canopy reflectance and the convergent properties
512 of plants. *New Phytol.*, 189, 375–394.
- 513 Palmer, M.W., Earls, P.G., Hoagland, B.W., White, P.S. & Wohlgemuth, T. (2002). Quantitative
514 tools for perfecting species lists. *Environmetrics*, 13, 121–137.
- 515 Pereira, H.M., Ferrier, S., Walters, M., Geller, G.N., Jongman, R.H.G., Scholes, R.J., *et al.*
516 (2013). Essential biodiversity variables. *Science*, 339, 277–278.
- 517 Pettorelli, N., Vik, J.O., Mysterud, A., Gaillard, J.-M., Tucker, C.J. & Stenseth, N.Chr. (2005).
518 Using the satellite-derived NDVI to assess ecological responses to environmental change.
519 *Trends Ecol. Evol.*, 20, 503–510.
- 520 Ricklefs, R.E. (2008). Disintegration of the ecological community. *Am. Nat.*, 172, 741–750.
- 521 Rocchini, D., Balkenhol, N., Carter, G.A., Foody, G.M., Gillespie, T.W., He, K.S., *et al.* (2010).
522 Remotely sensed spectral heterogeneity as a proxy of species diversity: Recent advances and
523 open challenges. *Ecol. Inform.*, 5, 318–329.
- 524 Rocchini, D., Luque, S., Pettorelli, N., Bastin, L., Doktor, D., Faedi, N., *et al.* (2018). Measuring
525 β -diversity by remote sensing: A challenge for biodiversity monitoring. *Methods Ecol. Evol.*, 9,
526 1787–1798.
- 527 Schmidtlein, S., Zimmermann, P., Schüpferling, R. & Weiß, C. (2007). Mapping the floristic
528 continuum: Ordination space position estimated from imaging spectroscopy. *J. Veg. Sci.*, 18,
529 131–140.

- 530 Schneider, F.D., Morsdorf, F., Schmid, B., Petchey, O.L., Hueni, A., Schimel, D.S., *et al.* (2017).
531 Mapping functional diversity from remotely sensed morphological and physiological forest traits.
532 *Nat. Commun.*, 8, 1441.
- 533 Schweiger, A.K., Cavender-Bares, J., Townsend, P.A., Hobbie, S.E., Madritch, M.D., Wang, R.,
534 *et al.* (2018). Plant spectral diversity integrates functional and phylogenetic components of
535 biodiversity and predicts ecosystem function. *Nat. Ecol. Evol.*, 2, 976–982.
- 536 Turner, W. (2014). Sensing biodiversity. *Science*, 346, 301–302.
- 537 Ustin, S.L. & Gamon, J.A. (2010). Remote sensing of plant functional types. *New Phytol.*, 186,
538 795–816.
- 539 Ustin, S.L., Gitelson, A.A., Jacquemoud, S., Schaepman, M., Asner, G.P., Gamon, J.A., *et al.*
540 (2009). Retrieval of foliar information about plant pigment systems from high resolution
541 spectroscopy. *Remote Sens. Environ.*, 113, 67–77.
- 542 Vellend, M. (2010). Conceptual synthesis in community ecology. *Q. Rev. Biol.*, 85, 183–206.
- 543 Wang, R. & Gamon, J.A. (2019). Remote sensing of terrestrial plant biodiversity. *Remote Sens.*
544 *Environ.*, 231, 111218.
- 545 Wang, R., Gamon, J.A., Cavender-Bares, J., Townsend, P.A. & Zygielbaum, A.I. (2018a). The
546 spatial sensitivity of the spectral diversity–biodiversity relationship: an experimental test in a
547 prairie grassland. *Ecol. Appl.*, 28, 541–556.
- 548 Wang, R., Gamon, J.A., Schweiger, A.K., Cavender-Bares, J., Townsend, P.A., Zygielbaum,
549 A.I., *et al.* (2018b). Influence of species richness, evenness, and composition on optical
550 diversity: A simulation study. *Remote Sens. Environ.*, 211, 218–228.
- 551 Whittaker, R.H. (1960). Vegetation of the Siskiyou Mountains, Oregon and California. *Ecol.*
552 *Monogr.*, 30, 279–338.

- 553 Whittaker, R.H. (1972). Evolution and measurement of species diversity. *Taxon*, 21, 213–251.
- 554 Woodcock, C.E. & Strahler, A.H. (1987). The factor of scale in remote sensing. *Remote Sens. Environ.*, 21, 311–332.

556 **TABLES**

557 **Table 1** Partitioning spectral diversity into additive components for the two simulated regions
 558 (Figs. 3–4) and for the NEON imagery (Fig. 5).

		High β, low α	Low β, high α	NEON imagery
				
Sums of squares (SS)				
SS_Y		1.66	1.66	740.24
SS_β (% of SS_Y)		1.40 (84.4%)	0.08 (4.8%)	168.85 (22.8%)
SS_α (% of SS_Y)		0.26 (15.6%)	1.58 (95.2%)	571.39 (77.2%)
Spectral diversity (SD)				
SD_Y		0.0027	0.0027	0.0029
SD_β		0.0022	0.00013	0.00065
\overline{SD}_α		0.00043	0.0026	0.0022
Feature contribution to SD (FCSD)				
$FCSD_Y$	PC 1	0.800	0.800	0.690

	PC 2	0.157	0.157	0.154
	PC 3	0.023	0.023	0.090
$FCSD_{\beta}$	PC 1	0.906	0.859	0.520
	PC 2	0.079	0.108	0.329
	PC 3	0.013	0.019	0.092
\overline{FCSD}_{α}	PC 1	0.259	0.798	0.733
	PC 2	0.513	0.158	0.108
	PC 3	0.050	0.022	0.092

559

560 **FIGURE LEGENDS**

561 **Figure 1** Partitioning plant spectral γ -diversity into additive β and α components. A region of
562 interest is split into a number of communities of a specific size and shape (here, 20 m \times 20 m
563 squares, representing standard forest inventory plots). Spectral γ -diversity refers to the total
564 spectral diversity in the entire region calculated from pixel-level reflectance. The β component
565 corresponds to spectral diversity *among* communities, with similar colours sharing more similar
566 spectral composition. The α component refers to spectral diversity *within* individual
567 communities. The left-most panel is a true colour (red-green-blue, RGB) image of an area of
568 Bartlett Experimental Forest; colours for the other panels were obtained using the reflectance of
569 different wavelength bands (R = 779 nm, G = 639 nm, B = 2301 nm), followed by linear
570 stretching.

571 **Figure 2** Overview of our proposed workflow for partitioning plant spectral diversity. In our
572 NEON case study, spectral data pre-processing included removing atmospheric water
573 absorption bands (wavelengths between 1340–1455 nm and 1790–1955 nm) and noisy regions
574 of the spectrum (wavelengths <400 nm and >2400 nm), and applying a Savitzky-Golay filter
575 (order = 3, size = 7) to every pixel in the image to remove high-frequency noise. We masked all
576 pixels with normalized difference vegetation index (NDVI) values <0.8, and brightness-
577 normalized all spectra (Feilhauer *et al.* 2010). Then, we performed a PCA with type I-scaling,
578 and visually inspected the first 17 PCs which together accounted for >99% of the total spectral
579 variation among all pixels (Fig. S3). Only the first five PCs showed meaningful biological spatial
580 patterns and were retained for spectral diversity measurements; PCs 6–17 were excluded
581 based on visual inspection as they expressed artefacts from image acquisition and processing
582 (Fig. S3). For illustration purposes, in the diversity partitioning analysis (bottom panel) we show
583 communities composed of only three pixels, whereas in fact we used a community size of 40 \times

584 40 pixels in our NEON case study. For abbreviations see text. *The shade mask is for illustrative
585 purposes and is not applied to the PCs shown in the middle panel.

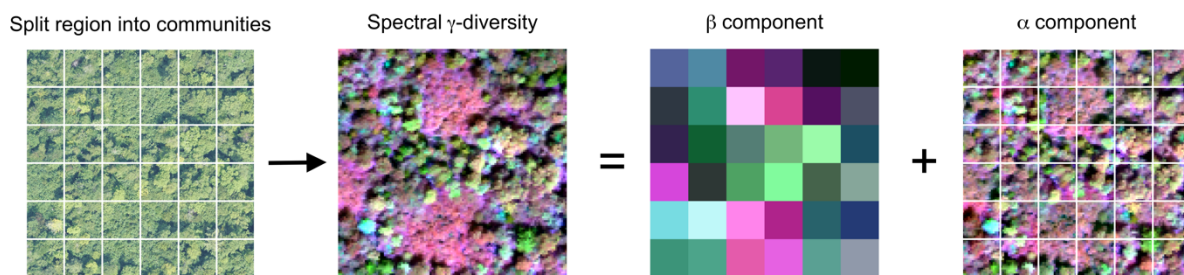
586 **Figure 3** Two simulated landscapes of equal spectral γ -diversity, but with contrasting spectral β -
587 diversity and α -diversity. **Left:** high spectral β -diversity but low α -diversity. **Right:** low spectral β -
588 diversity but high α -diversity. Each landscape is composed of 25 communities (numbered black
589 squares), each composed of 5×5 pixels (smaller coloured squares). The size of each pixel is
590 equivalent to the size of an individual plant and their colour corresponds to one of the 15 leaf
591 spectra (= 3 species \times 5 individuals) shown in Figure S1. These colours were set by mapping
592 the scores of the first three principal components (PC) for each spectrum to a red-green-blue
593 (RGB) scale (PC 1 = green, PC 2 = red, PC 3 = blue). We generated the high spectral β -
594 diversity but low spectral α -diversity scenario (left panel) by randomly assigning (with
595 replacement) pixels within each community with individual spectra from single species (Fig. S1,
596 bottom row). We selected species identity per community at random using the following
597 probabilities: 0.60 (*Betula alleghaniensis*, green hues), 0.35 (*Populus deltoides*, blue hues) and
598 0.05 (*Populus tremuloides*, red hues). In this scenario, spectral β -diversity was high and spectral
599 α -diversity low because interspecific spectral variation (particularly between *Betula* and the two
600 *Populus* species) was higher than intraspecific spectral variation (Fig. S2). Next, to reduce
601 spectral β -diversity and increase α -diversity while holding γ -diversity constant, we moved the
602 pixels of the left panel to randomly selected positions in the right panel.

603 **Figure 4** (a) Spectral α -diversity (SD_α), (b) local contribution to spectral β -diversity ($LCSD_\beta$), and
604 (c-d) feature contribution to spectral α -diversity ($FCSD_\alpha$) for the first two spectral features (i.e.
605 first two principal components of the brightness-normalized reflectance data) of each community
606 in the two simulated regions. PC = principal component.

607 **Figure 5** Partitioning spectral diversity using imaging spectroscopy data acquired by the
608 National Ecological Observatory Network (NEON) over the Bartlett Experimental Forest site.
609 From left to right: (1) true colour (red-green-blue, RGB) image with 0.1 m ground resolution, (2)
610 false colour image with 1 m resolution based on the first three principal components (PCs) of
611 the spectral image cube (PC1 = red, PC2 = green, PC3 = blue), (3) local contribution to spectral
612 β -diversity (LCSD $_{\beta}$), and (4) spectral α -diversity (SD $_{\alpha}$) of forest communities, each measuring 40
613 m \times 40 m. For panels 3 and 4, light hues correspond to low, dark hues to high values of LCSD $_{\beta}$
614 coefficients and SD $_{\alpha}$ values, respectively.
615

616 **FIGURES**

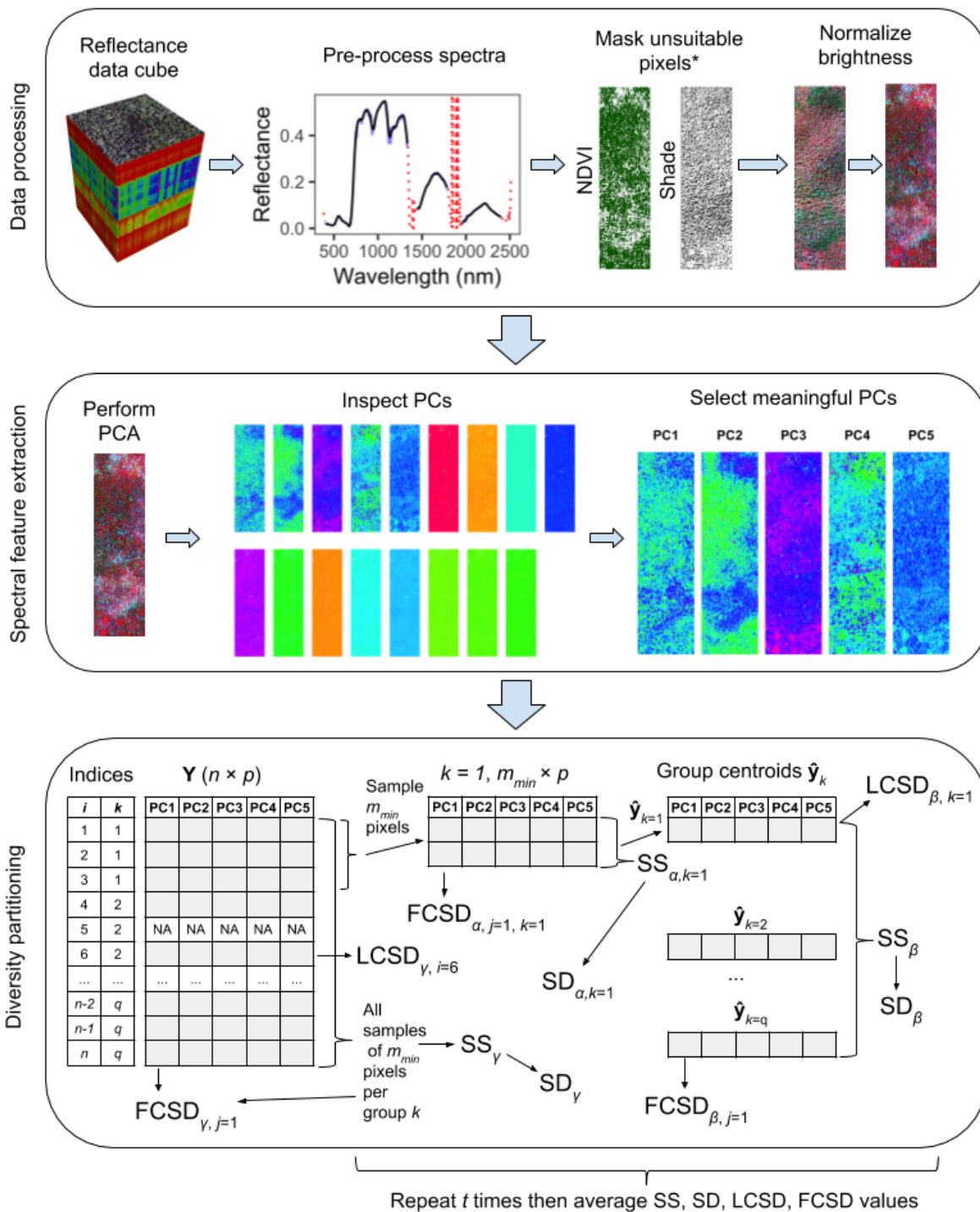
617 **Figure 1**



618

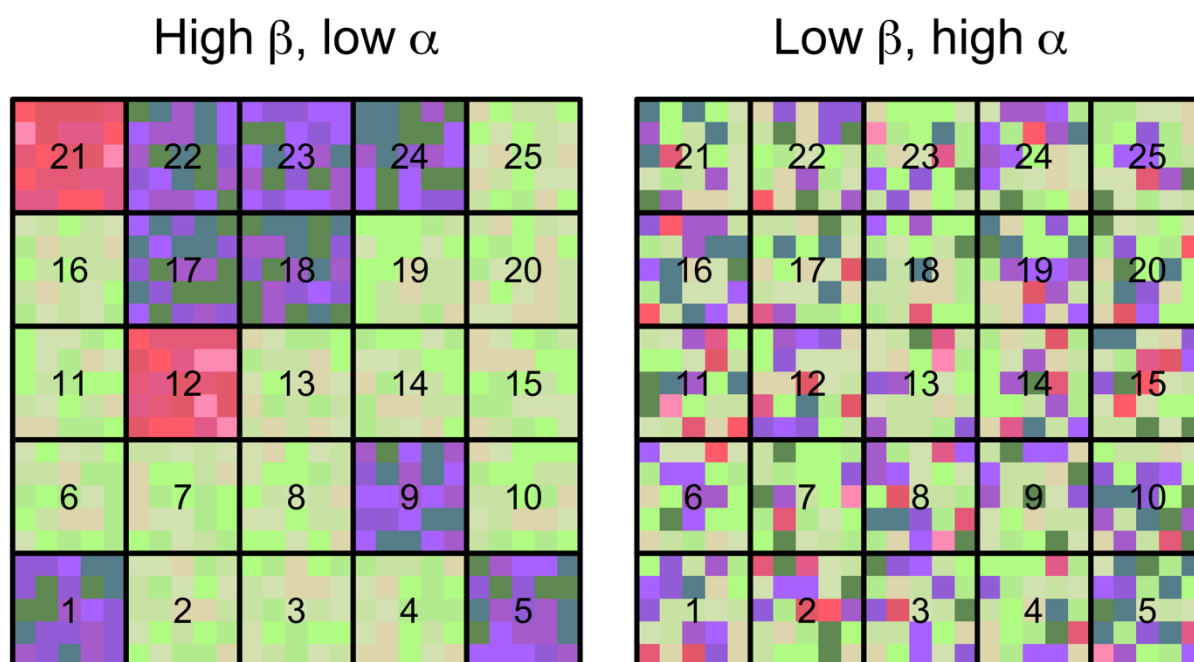
619

620 **Figure 2**



621

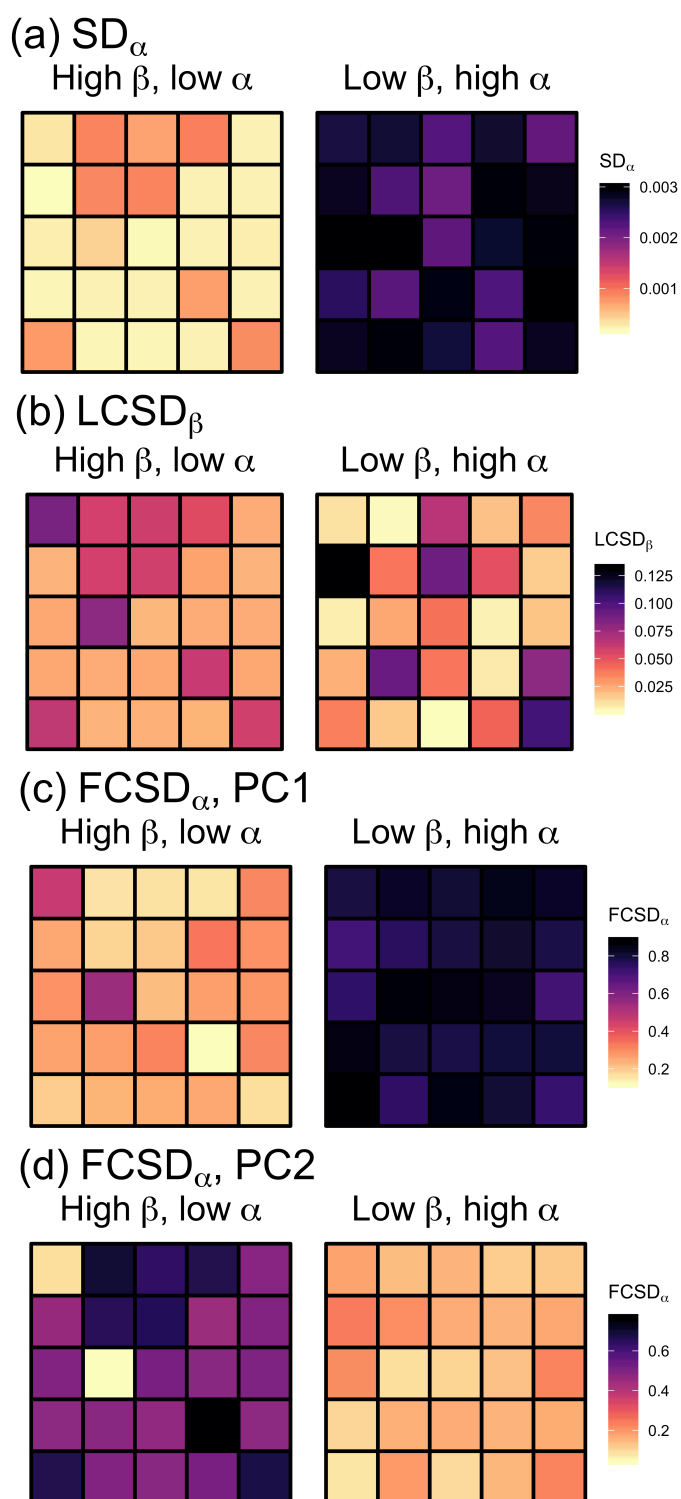
622 **Figure 3**



623

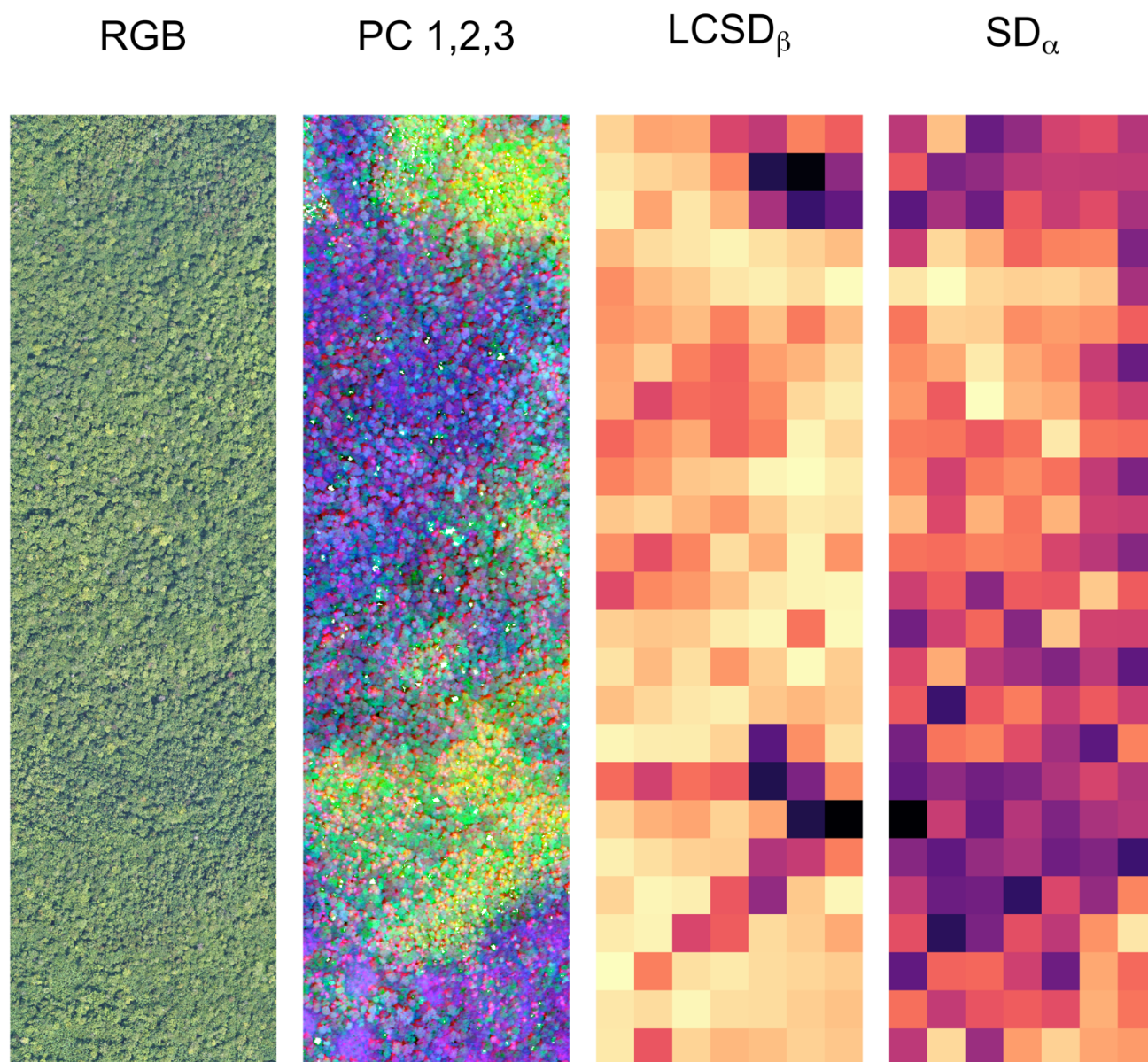
624

625 **Figure 4**



626

627 **Figure 5**



628